Using corrugated tubes in external molten salt receivers

Cite as: AIP Conference Proceedings **2126**, 030061 (2019); https://doi.org/10.1063/1.5117573
Published Online: 26 July 2019

Ralf Uhlig, Cathy Frantz, and Reiner Buck

Using Corrugated Tubes in External Molten Salt Receivers

Ralf Uhlig[1, a)], Cathy Frantz[2] and Reiner Buck[3]

[1]*Team manager Receiver Development, German Aerospace Center (DLR), Institute of Solar Research, Pfaffenwaldring 38-40, Stuttgart, Germany*
[2]*Researcher, German Aerospace Center, Institute of Solar Research, Pfaffenwaldring 38-40, 70567 Stuttgart, Germany*
[3]*Head of department Solar Tower Systems, German Aerospace Center, Institute of Solar Research, Pfaffenwaldring 38-40, 70567 Stuttgart, Germany*

[a)]Corresponding author: ralf.uhlig@dlr.de

Abstract. CFD models have been used to show the potential of using corrugated tubes instead of smooth tubes at a solar thermal receiver using molten salt as heat transfer fluid. The results were compared on the basis of a 700 MW_{th} receiver. Absorber tubes with an inner diameter between 32.8mm and 70 mm using a helical ribbed structure have been analyzed. The results show that a positive effect can only be achieved for configurations where the fluid velocity is lower than for the base hydraulic design with a fully developed turbulent flow. The presented approach proposes therefore tubes with larger inner diameter and reduced fluid velocity and pressure drop. The difference in pressure drop to the base design can then be used to introduce a swirl flow which leads to better mixing of the fluid and therefore lowers the temperatures of the tube wall, the fluid and also the thermal gradients. Corrugated tubes can be used to add an additional design parameter for a thermo-hydraulic optimization of the receiver.

INTRODUCTION

One major advantage of molten salt systems is that the molten salt can be used as heat transfer and storage medium. The receiver itself is the key component of solar thermal tower systems. Within the receiver the concentrated solar radiation is absorbed and transferred to the heat transfer media. In case of molten salt receivers the heat transfer fluid is pumped through a number of absorber tubes which are arranged in panels building a cylindrical shape, in parallel and serial configuration.

RECEIVER DESIGN

Introduction

One strong boundary condition in tubular receiver system design is the adherence to a modular panel design. This requirement leads to a discrete number of identical panels. Further basic design parameters are the thermal rating, the mean flux density, the maximum allowable pressure drop, tube dimensions (diameter, length), the interconnection between the panels and the aspect ratio (aperture height/diameter). An optimal receiver design is a compromise between all parameters.

HPMS 700 MW_{th} Molten Salt Receiver

Within the HPMS (High Performance Molten Salt) project different receiver concepts for a 700 MW_{th} molten salt system have been evaluated [1]. The ASTRID code [2] was used for the design of the receiver by optimizing the thermo-hydraulic layout in a first step. On the basis of this design the code was used to generate a thermal finite

SolarPACES 2018
AIP Conf. Proc. 2126, 030061-1–030061-8; https://doi.org/10.1063/1.5117573
Published by AIP Publishing. 978-0-7354-1866-0/$30.00

element (FE) model of the receiver considering the absorber tubes, the insulation and radiation protection. The model considers local heat transfer to the heat transfer fluid by using 1D fluid elements. The heat transfer coefficient is calculated according to the hydraulic boundary conditions of the receiver using the Gnielinski Nusselt correlation. The local solar heat flux distribution is considered by raytracing on the FE mesh. Infrared radiation exchange between components and convective and radiative losses to ambient complete the thermal boundaries. This model allows detailed simulation of the thermal field of the components for different load situations. Figure 1 (a) and (b) show the model and an example of the locally resolved thermal field.

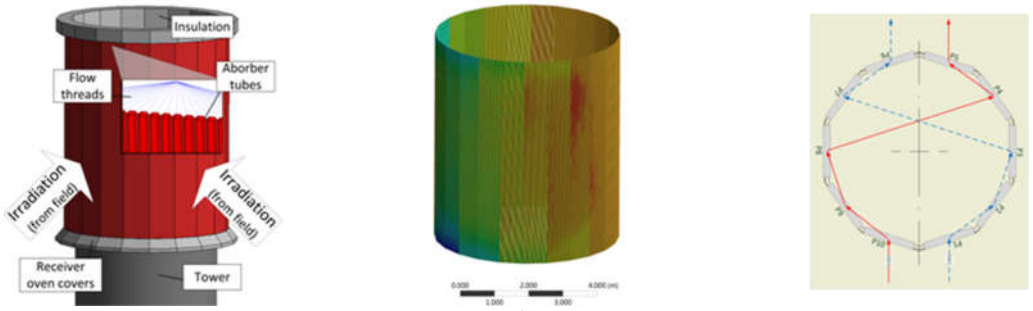

(a) (b) (c)

FIGURE 1. ASTRID© receiver model; (b) thermal field calculated, (c) interconnection (north is top);

The basis of the results presented in this paper is the design of the HPMS 700MW$_{th}$ receiver. The mass flow is divided into two passes (see Fig. 1 (c)) each with 5 panels connected in series. Table 1 gives the main data of the receiver. Thermal values are given for design point conditions.

TABLE 1. Input data for the CFD model

Parameter	Unit	
Thermal power	[MW]	696.4
Inlet temperature	[ºC]	290
Outlet temperature	[ºC]	565
Inlet pressure	[bar]	13
Mass flow	[kg/s]	1729.3
Number of Panels	[-]	10
Tubes per panel	[-]	141
Irradiated tube length	[m]	25.7
Inner diameter of tubes	[mm]	32.8

Using Corrugated Tubes to Enhance Heat Transfer Coefficient

Spirally grooved tubes have been used in various industrial fields such as electric power generation, refrigeration, chemical engineering, and have been widely investigated in available literature. The performance of heat exchangers can be improved by using surface modification or additional devices incorporated into the equipment. Transverse or helical repeated ribs are an attractive way of creating the surface roughness due to the inexpensive manufacturing. Depending on the manufacturing technique, ribs are found in several configurations. Fig. 2 shows sketches of several types of ribbed tubes along with the geometrical parameters involved.

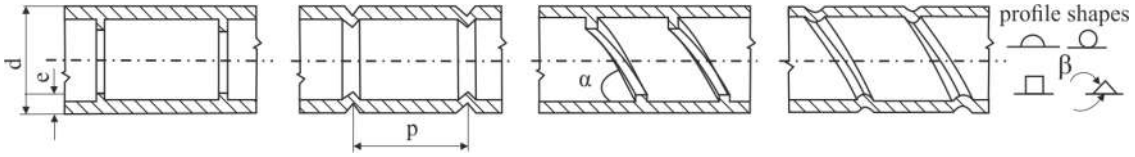

FIGURE 2. Configurations used in [6]

Within the SOLHYCO project a wire coil insert was used to enhance the heat transfer of a tubular air receiver [3]. The wire coil was manufactured specifically for this receiver. A significant additional effort was the correct placement of the wire coil in the absorber tubes. Besides this, the correct position of the wire coil cannot be checked easily after installation. Furthermore, there is no defined connection between tube wall and the wire coil. Heat transfer enhancement within turbulent flows is mostly effective when only the viscous boundary layer is mixed. Any type of insert that mixes the core flow (twisted tape, mesh or brush inserts) will not significantly enhance the heat transfer in a turbulent flow, but increase pressure drop [4] [5].

Ravigururajan et al. [6] have developed general correlations for friction factors and heat transfer coefficients for single-phase turbulent flow in internally augmented tubes. For this purpose data from previous research has been gathered for a wide range of tube parameters (e/d from 0.01 to 0.2; p/d from 0.1 to 7.0; α from 27° to 90°) and flow parameters (Re from 5000 up to 250000 and Pr from 0.66 to 37.6). The considered experimental data was based on different tube enhancements using different fluids (water, air, N_2, He). The resulting equations are

The developed correlation for the friction factor predicted 77% of the data within +/- 20%. The correlation for heat transfer predicted 69% within +/-20%. Furthermore they analyzed the influence of the different roughness parameters on the friction factor and heat transfer using the developed correlation. They found roughness height (e/d) values > 0.04 causes a much greater increase in friction than heat transfer. The pitch (p/d) has a similar effect on both friction and heat transfer. In contrast, the helix angle α has a similar effect on both parameters up to values <0.4. For values greater than 0.4 the effect on friction is much greater than the effect on heat transfer. The increase of friction finally stabilizes around 0.7.

Several patents have been filed by different authors for the use of enhanced tubes in central solar receivers: in 1996 Boeing Co. filed a patent on the usage of twisted-tape inserts for solar receivers [7] The invention aims at reducing the size of the receiver by increasing the heat transfer inside the tube while promising a parallel reduction of pressure losses. Twist staging is designed to provide a higher heat transfer coefficient in the receiver's central region where the solar flux is high and a reduced pressure loss at the low solar flux entrance and exit end regions. In 2011 the Siemens AG applied for a patent for a solar collector of a solar parabolic through steam generator comprising an absorber tube which has a spirally shaped rib on its inner side [8]. The internally grooved tubes cause the flow to swirl, which leads to the separation of water and steam phase. The water is forced against the pipe wall, so that the heat transfer characteristics are improved.

Jiangfeng et al. [9] experimentally investigated the transition and turbulent convective heat transfer performance of molten salt in spirally grooved tubes as a function of Reynolds number (5000-15000) and relative groove height using the nitrate salt mixture (KNO_3-$NaNO_2$-$NaNO_3$). The investigated inlet temperatures of the molten salt ranged between 200 and 350°C, the applied heat flux was about 250-260 kW/m² . They found good agreement between their experimental results for a smooth tube and the Gnielinksi and Sieder-Tate correlations. Furthermore they deduced a correlation for the Nusselt number both for turbulent and transition flow for spirally grooved tubes based on their experimental results. This correlation was however not compared to the more general correlation of Ravigururajan et al..

Lu et al. [10] investigated the impact of spirally grooved pipes on the Nusselt number. They deduced a generalized correlation for both non-enhanced and spirally grooved tubes for Reynolds numbers ranging between 1000 and 10’000. They compared the proposed correlation to existing data from smooth tube measurements for different molten salts, as well as to their own experimental data for spirally grooved tubes with different groove height to pipe diameter ratios. Furthermore they evaluated the experimental temperature difference between absorber inner wall and the used Hitec salt mixture. They were able to show that the temperature gradient expected in a smooth tube can be decreased by about 30°C by using a spirally grooved tube with the highest e/d ratio for Re=5400. At Reynolds numbers around 13’000 the temperature gradient can only be reduced by 14°C.

CFD MODELLING

Quality Assurance

The quality of the CFD simulations was ensured by mesh studies for the highest Reynolds number for every model. The discretization error for the presented results is less than 1 % in reference to the infinitesimal mesh. The distance of the first fluid node to the wall was chosen to be $1 \cdot 10^{-8}$ m to guarantee an average dimensionless wall distance (y^+) < 1. The Shear Stress Transport (SST) turbulence model and temperature dependent material properties were used for all simulations. All simulation residuals reached values < $1 \cdot 10^{-7}$.

Comparison Between CFD and Thermal Receiver Model (ASTRID)

As a first step a CFD model of the fluid of one absorber tube was used to analyze the thermal gradient within the fluid caused by the inhomogeneous heat input and the results were compared to the results of the ASTRID thermal receiver model. The base for this analysis was the above described HPMS 700 MW_{th} receiver. The tubes with the highest heat flux of an inlet and outlet panel was chosen for the model. The heat flux distribution was modelled on the fluid outside as net heat flux transferred to the fluid from the ASTRID receiver model (Fig. 3).

At the inlet, the mass flow, the inlet temperature and a static pressure at the outlet was modelled as flow boundaries. Table 2 gives an overview on the boundaries of the CFD model.

TABLE 2. Input data for the single tube CFD model

Parameter	Unit	Tube of inlet panel	Tube of outlet panel
Mass flow	[kg/s]	6.132	
Inlet temperature	[ºC]	290	531.7
Maximal heat flux	[kW/m^2]	811.7	343

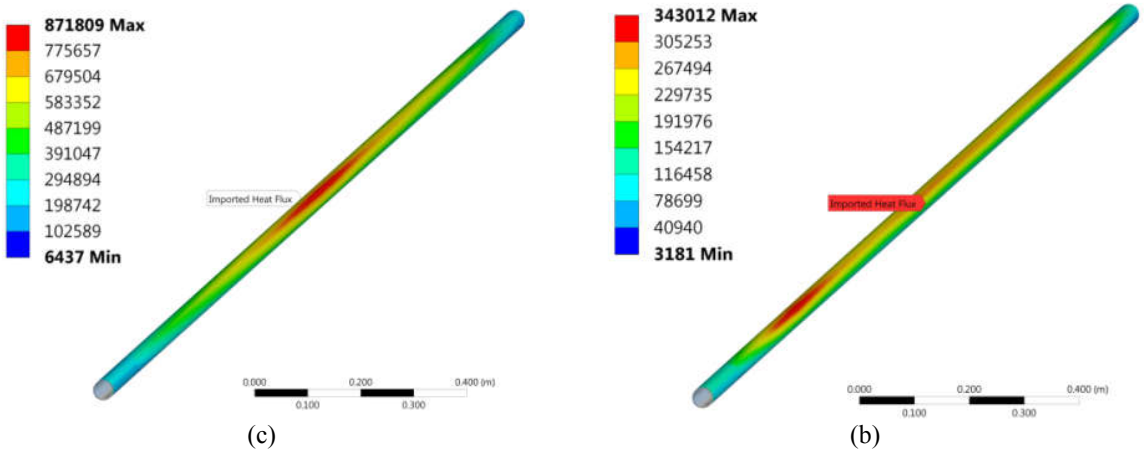

FIGURE 3. Net heat flux [W/m^2] to the fluid for the tube of an inlet panel (a) and outlet panel (b).

The results of the CFD model are listed in Table 3. The model representing the inlet panel shows a maximal thermal gradient up to 61.7 K. At the outlet panel the gradient is lower (23.2 K) due to the lower heat flux.

The reason for the lower used heat lux at the outlet panel is to prevent overheating of the fluid in order to avoid decomposition of the salt and increased corrosion of the absorber tubes. The result of the CFD model shows a maximal film temperature of 580 °C which is still acceptable. The maximal absorber temperature given by the CFD model are higher than predicted by the ASTRID© receiver model due to the higher film temperatures at the regions with higher heat flux.

TABLE 3. Comparison of CFD and ASTRID© receiver model

Topic	Unit	Tube of inlet panel		Tube of outlet panel	
		CFD	ASTRID©	CFD	ASTRID©
Heat transferred to fluid	[kW]	704.1	704.1	313.2	313.2
Average fluid temperature at outlet	[ºC]	367.1	368.9	566.6	566.1
Maximal fluid temperature	[ºC]	390.1	368.9	580.3	566.1
Maximal temperature gradient in fluid	[K]	61.7	N/A	23.2	N/A

CFD Analysis of Helical Ribbed Tubes

Model Assumptions

The CFD models consider the fluid and the tube with a length of one meter. The wall thickness of the tube was set to 1.5mm for all variations. The heat flux on the tube outside was modeled using a similar circumferential distribution as in reality but homogenous along tube length (see (1) and Fig. 4). Radiation exchange between neighbor tubes, radiative and convective losses were neglected as the aim of this investigation was the comparison of the different tube dimensions. An inlet temperature of 290 °C and the mass flow were set as the inlet boundary. At the inlet also a velocity distribution of a previous (isothermal) flow simulation was used to establish a full developed flow at the inlet. At the outlet an average static pressure was set as boundary.

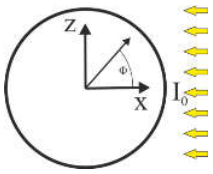

$$\dot{q} = I_0 \frac{x}{\sqrt{x^2+z^2}} \quad (1)$$

FIGURE 4. Net heat flux distribution

Parameter Study of Helically Ribbed Structure

The corrugated tube design using helical ribs was chosen for a parametric study of the geometry parameters of the structure. An inner diameter of 32.8 mm and a mass flow of 6.132 kg/s, which corresponds to the HPMS 700 MW_{th} receiver, were used for this analysis. An absorbed heat flux (I_0) of 685kW/m^2 was modelled. The pitch (p) and the rib height (e) were varied. The maximal tube wall and fluid temperatures, the maximal thermal gradient within the fluid and the pressure drop were evaluated and compared to the smooth tube of the base receiver (see Table 4)

TABLE 4. Comparison of smooth tubes with varied corrugated tube designs

Topic	Unit	Smooth tube	Corrugated tube								
Pitch (p)	[mm]	-	50	100	200	50	100	200	50	100	200
Rib height (e)	[mm]	-	2	2	2	5	5	5	8	8	8
Tube temperature	[ºC]	391.4	382.8	382.6	388.6	384.1	379.2	385.7	379.7	371.7	388.6
Fluid temperature	[ºC]	342.8	332.3	331.4	336.2	324	327.5	331.7	318.3	323.5	333.2
Thermal gradient	[K]	52.8	42.3	41.4	46.2	34	37.5	41.7	28.3	33.5	43.2
Pressure drop	[mbar]	30	56.4	40.6	35.1	371.5	137.1	67.2	1139	296.2	104.9

The results show that the effect of reducing the temperatures and the thermal gradients is very small in comparison to the increase in pressure drop, which means a significant increase of pumping power. Highest reduction of temperatures can be achieved with pitch of 50mm and a rib height of 8 mm with the penalty of a nearly 38 times higher pressure drop. The reason for these results is that the flow is already fully turbulent and therefore is the effect of increasing the heat transfer is not very pronounced.

Helically Ribbed Tubes with Lower Fluid Velocity

As shown in the previous chapter, the usage of helically ribbed tubes is not very promising if the approach is applied to a thermo-hydraulic layout designed already for a fully developed turbulent flow. The disproportionately increasing pressure loss is not desirable. However, the effect might be more advantageous if the average fluid velocity and pressure drop is reduced.

To demonstrate this approach again the HPMS receiver design was taken as the base design. The dimensions of the receiver and panels as well as the interconnection between panels are seen as fix. The only freedom is then increasing the diameter and consequently reducing the number of parallel absorber tubes per panel (with panel width

remaining the same). Even if the mass flow is then split to less parallel tubes, the fluid velocity and the pressure loss would decrease due to the quadratic increase of flow cross section. The gap in pressure drop (in comparison to the original design) could then be used to introduce the swirl flow with the aim to enhance mixing of the fluid and so lowering the maximal temperatures and thermal gradients within the fluid.

Different tube diameters were analyzed and the dimensions of the helical rib geometry (p, e) were optimized. Aim was the maximal possible reduction of temperature and gradients with a pressure loss similar or lower than the base configuration.

Figure 5 shows the temperature distribution within the fluid for the smooth tube with Di = 32.8mm (a) and the helical ribbed tube Di=50 mm, p=200mm, s=10mm (b). The effect of the swirl flow can be seen in in Fig. 5. (c).

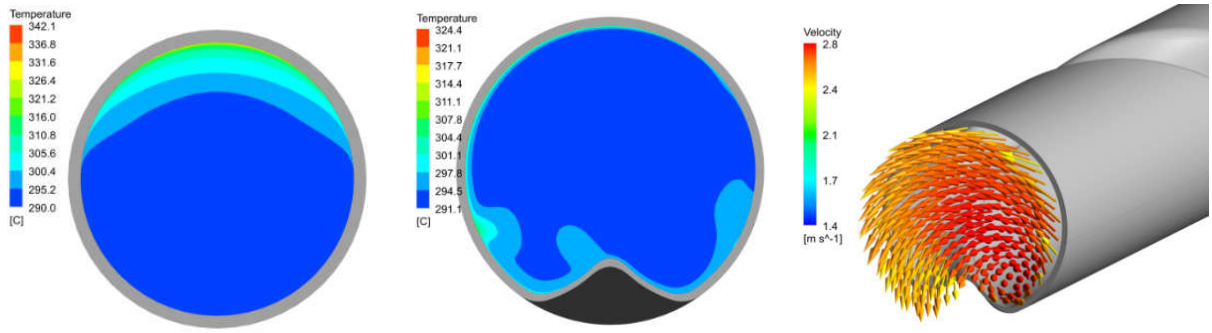

(a) (b) (c)

FIGURE 5. Fluid temperature smooth tube (Di=32.8 mm); fluid temperature helical ribbed tube (Di=50 mm, p=200mm, s=10mm (b); velocity at outlet helical ribbed tube (Di=50 mm, p=200mm, s=10mm)

The results of this analysis are listed at Table 5. The geometric design of the helical ribbed tube versions (groove depth and pitch) presented here are the ones showing lowest maximal fluid temperature and gradient with a pressure drop similar or lower than the base design. It can be seen that for every larger tube diameter a positive effect can be achieved. The highest reduction of temperature and gradient could be reached with tubes with an inner diameter of 50 mm.

TABLE 5. Comparison of smooth and helically ribbed tubes

Parameter	Unit	Smooth tube	Helically ribbed tube		
Inner diameter	[mm]	32.8	50	60	70
Number or parallel tubes	[pcs]	141	93	77	66
Maximal fluid temperature	[°C]	342.8	323.5	328.7	336.2
Maximal temperature gradient in fluid	[K]	52.8	33	38	46
Maximal tube temperature	[°C]	391.4	386.6	389.4	393.8
Pressure drop	[mbar]	30	28.7	29.9	26.6
Groove depth (s)	[mm]	-	200	200	50
Pitch (p)	[mm]	-	10	12	4

OUTLOOK AND CONCLUSIONS

Outlook

Test Rig for Heat Transfer Measurement

Thermomechanical analysis is fundamental in sizing of the receiver surface during plant design and in the establishment of operational heat flux limits for heliostat field control. This requires an accurate estimate of the convective heat transfer coefficient on the medium side of the tube, typically done by using correlations for heat transfer in turbulent flow. However process flow conditions in molten salt receiver tubes exceed the experimentally explored range of Reynolds number for molten salts both for smooth and enhanced tubes by a large margin. Das et al. [11] found that at lower Reynolds number conditions, the available experimental molten salt heat transfer data followed the commonly used correlations for smooth tubes [12], [13]. However, in the region of interest for practical receiver design (Re>50'000), the correlations overestimate the experimentally determined heat transfer data by a factor of up to 3. An analytical study has shown that the observed effects would lead to an increase of absorber temperatures by up to 170°C. For this reason DLR is currently developing a test loop for experimental investigations on heat transfer of Solar Salt ($NaNO_3$-KNO_3) in both smooth and enhanced tubes. This test setup will be using the infrastructure of the TESIS test bed located in Cologne, Germany [14]. The results of the experimental campaign will be compared to the developed CFD simulation in order to validate the model.

Improved Receiver Design Using Corrugated Tubes

The chosen design for the analyzed corrugated tubes (helical ribs) might not be the structure with the best performance. Aim of this paper was to show the potential of this approach. After validation of the CFD model at the abovementioned heat transfer test loop, CFD can be used to analyze different kinds of corrugated tube designs. But even the presented structure of helical ribs can be used in several variations. The rib height and pitch can be optimized regarding swirl effect and allowable pressure drop not only as one design for the complete receiver. For example the rib height and the pitch could vary over the tube length for example to adapt the effect of the swirl flow to the heat flux distribution (high flux = high swirl effect) (Fig. 6). This also means that not every tube of the receiver must have the same parameters for groove depth and pitch (Fig. 7). Furthermore a partial corrugated geometry could introduce the swirl only in regions where it is beneficial. In the end all this variations could be combined to tailor the tubes according to the load situation in the receiver (Fig. 8). As the different structures will lead to different pressure drop it could then be necessary to homogenize the mass flow distribution by adding additional pressure drop at tubes with less aggressive structures or if corrugated tubes are combined with smooth tubes. Last but not least the optimal design can only be determined by comparing the levelized cost of electricity. Therefore the complete system performance and costs of all components must be taken into account.

FIGURE 6. Helical ribs witch variable pitch and groove depth along tube length

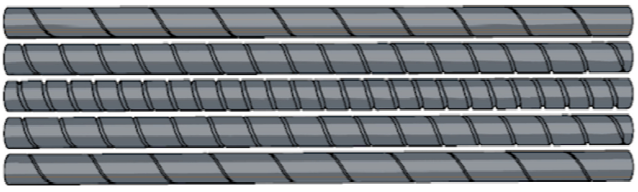

FIGURE 7. Tailored receiver panel using different geometry of corrugated tubes

FIGURE 8. Partial helical ribs

Conclusion

A CFD model has been used to analyze the thermal gradients and maximal fluid temperatures of a 700 MW_{th} tubular molten salt receiver at an inlet and outlet panel using the local heat transfer of the detailed receiver model.

The CFD model of a helically ribbed tube was used to perform a parameter study with the base configuration of a 700 MW_{th} thermal receiver. It was found that the usage of helically ribbed tubes is not very promising if the approach is applied to a thermo-hydraulic layout designed already for a fully developed turbulent flow. The disproportionately increasing pressure loss is not acceptable.

Then an approach with reduced average velocity of the fluid was presented. The smooth tubes of the base 700 MW_{th} thermal receiver were replaced by helically ribbed tubes with increased diameter without changing other parameters of the receiver (size, interconnection, mass flow, flux). The number of parallel tubes was adapted to the panel width. For all analyzed tube diameters a helical rib structure could be found showing a positive effect regarding lowering the temperatures and thermal gradients without increasing the pressure loss. The geometric parameters of the helical rib structure were optimized by varying the rib height and the pitch.

In conclusion, this approach opens a new design parameter for molten salt receiver optimization. By varying the structure and parameters of corrugated tubes, the design can be tailored to local boundaries (flux distribution, fluid temperature). Furthermore the reduction of the film temperature could open a path to higher salt outlet temperatures. After the validation of the CFD model in a test bench which is currently under development, the model can be used for intense parameter studies and could allow the enhancement of tubular receivers.

REFERENCES

1. M. Puppe, *Techno-Economic Optimization of Molten Salt Solar Tower Plan*t (SolarPACES 2017, 26.-29. Sept. 2017, Santiago de Chile)
2. C. Frantz, *ASTRID© – Advanced Solar Tubular ReceIver Design: A Powerful Tool for Receiver Design and Optimization*. (AIP Conference Proceedings. SolarPACES 2016, 11.-14.1 Okt. 2016, Abu Dhabi, AE)
3. L. Amsbeck, et.al., *Development of a tube receiver for a solar hybrid microturbine system*, Proc. SolarPACES 2008, Las Vegas, USA (2008)
4. Webb, R.L.; Eckert, E.R.G.; Goldstein, R.J.: *Heat Transfer and Friction in Tubes with Repeated-Rib Roughness*, Int. J. Heat and Mass Transfer, Vol. 14, S. 601-617, 1971
5. D. L. Davids, "Recovery effects in binary aluminum alloys," Ph.D. thesis, Harvard University, 1998.
6. T.S. Ravigururajan, A.E. Bergles, *Development and verification of general correlations for pressure drop and heat transfer in single-phase turbulent flow in enhanced tubes*. Experimental Thermal and Fluid Science 13 (1996) 55–70
7. DE102011004266A1
8. US5850831A
9. Jiangfeng Lu. et al., *Enhanced heat transfer performances of molten salt receiver with spirally grooved pipe*, (Applied Thermal Engineering 88 (2015) 491-498)
10. J.F. Lu, X.Y. Sheng, J. Ding, J.P. Yang, *Transition and turbulent convective heat transfer of molten salt in spirally grooved tube*. Exp. Therm. Fluid Sci. 47 (2013) 180-185
11. A. Das, *Heat Transfer Behavior of Molten Nitrate Salt*. AIP Conference Proceedings 1734, S. doi: 10.1063/1.4949094.
12. F. Dittus and L. Boelter, Int. Commun. Heat Mass Transf. 12, 3-22, pp. 3-22, 1985
13. V. Gnielinski, *Int. Chem. Eng. 16,* pp. 359-368, 1976
14. Odenthal, Christian und Klasing, Freerk und Bauer, Thomas *Demonstrating Cost Effective Thermal Energy Storage in Molten Salts: DLR's TESIS Test Facility*. Energy Procedia, 135, Pages 14-22. EIsevier. DOI: 10.1016/j.egypro.2017.09.483 ISSN 1876-6102, (2017)